Asymmetric Distribution of Cooperativity in the Binding Cascade of Normal Human Hemoglobin. 2. Stepwise Cooperative Free Energy†

Jo M. Holt and Gary K. Ackers*

Department of Biochemistry & Molecular Biophysics, Washington University School of Medicine, 660 South Euclid Avenue Box 8231, St. Louis, Missouri 63110

Received April 18, 2005; Revised Manuscript Received June 8, 2005

ABSTRACT: Stepwise cooperative free energies and intermediate Hill coefficients are used to assess the presence of noncooperative sequences in the database of binding free energies previously obtained for the eight partially ligated intermediates of human hemoglobin, encompassing a variety of hemesite analog substitutions. This analysis is prompted by the observed noncooperative binding of two ligands to hemoglobins that are partially substituted with Zn^{2+}-heme, an analog of deoxy Fe^{2+}-heme (Holt et al. (2005) *Biochemistry 44*, XXXXX). The results show that noncooperative binding sequences are observed in all hemesite analog studied to date. The noncooperative binding observed in ($\alpha^2Zn\beta^2FeO_2$) and ($\alpha^2FeO_2\beta^2Zn$) is therefore not a Zn-specific substitution artifact. One of several binding sequences from singly to triply ligated hemoglobin is also observed to occur with little or no positive cooperativity. These results demonstrate the variability possible among different ligation pathways in a highly cooperative multi-subunit system such as hemoglobin. As a direct consequence of this variability, differences among ligation pathways are not always detectable using cooperativity functions based on statistical distributions, such as the Hill coefficient n_H. The limitations of Hill coefficient analysis in evaluating cooperativity in intermediates of complex systems is contrasted with the utility of the stepwise binding parameters.

In the course of binding four oxygens, the human hemoglobin tetramer (Hb)[1] assumes a total of eight partially ligated intermediates, or microstates. Through the binding free energies of each microstate, a detailed picture of the Hb cascade (Figure 1) is emerging in which the $\alpha\beta$ dimer within these microstate tetramers acts as a functional, cooperative unit. The foundation of these recent ideas has been built on two experimental observations. The first is that binding the second ligand to the tetramer occurs with a higher affinity when ligation occurs on the same dimer, in contrast with the three other doubly ligated tetramers bearing a ligand on both $\alpha\beta$ dimers (Figure 1) (reviewed in ref *1*). Of the four unique configurations of bound ligand in doubly ligated Hb, the most thermodynamically stable (by an order of magnitude) is that in which one dimer is fully ligated and the other remains deoxy. This asymmetric distribution of binding affinity (and cooperativity) at the second binding step has been observed in a variety of hemesite analogs at equilibrium (*1*−*3*), and in CO binding kinetics in wild type (*4*) and analog Hb (*5*), and is therefore concluded to be a real property of Hb rather than an artifact of any particular analog.

A second robust observation concerns the effect of classical mutations and chemical modifications of residues in the dimer−dimer interface. When the modification is applied asymmetrically, i.e., to only one of the dimers within the tetramer, the subsequent alteration of the binding constant is confined to the modified dimer (*6*). No significant change to ligand binding in the wild type partner dimer is detected. These classical modifications have historically been thought to exert their influence on dimer−tetramer assembly free energies, ligand binding constants, and cooperativity by weakening the dimer−dimer interface, thereby simultaneously affecting all hemesites in both dimers. By contrast, however, asymmetric modifications demonstrate that the perturbation of the dimer−dimer interface is not communicated to both dimers within the tetramer. Like the first observation described above, in which different binding free energies for the second ligation step were found, the asymmetric response of the tetramer to asymmetric mutation points to the $\alpha\beta$ dimer within the tetramer as a source of communication leading to cooperativity.

As demonstrated in the previous paper (*7*), some binding sequences within the cascade can occur without significant cooperativity (*7*, *8*). This finding is particularly nonintuitive: given the strong positive cooperativity observed in the overall binding isotherm, it seems likely that each successive binding event in the Hb cascade would exhibit positive cooperativity. The fact that noncooperativity is not a generally recognized feature of Hb binding requires a closer examination of the sequence of binding steps in the overall cascade, particularly with reference to the possibility of a Zn-substitution artifact.

In this report, the existing database of stepwise binding free energies that comprise the Hb binding cascade are assessed for stepwise cooperativity in order to ascertain the extent to which noncooperative sequences in the cascade are a general phenomenon, independent of the specific hemesite analog employed. The results of this comparison show that ligation of a deoxy dimer within a tetramer already containing a single ligand on the partner dimer occurs with no significant cooperativity, regardless of the hemesite analog. In addition,

† This work was supported by grants from the National Institutes of Health (GM24486) and the National Science Foundation (MCB0077596).

* Author to whom correspondence should be addressed. E-mail: ackers@wustl.edu. Phone: 314-362-0260. Fax: 314-747-3467.

[1] Abbreviations: Hb, hemoglobin.

10.1021/bi050710n CCC: $30.25
Published on Web 08/16/2005

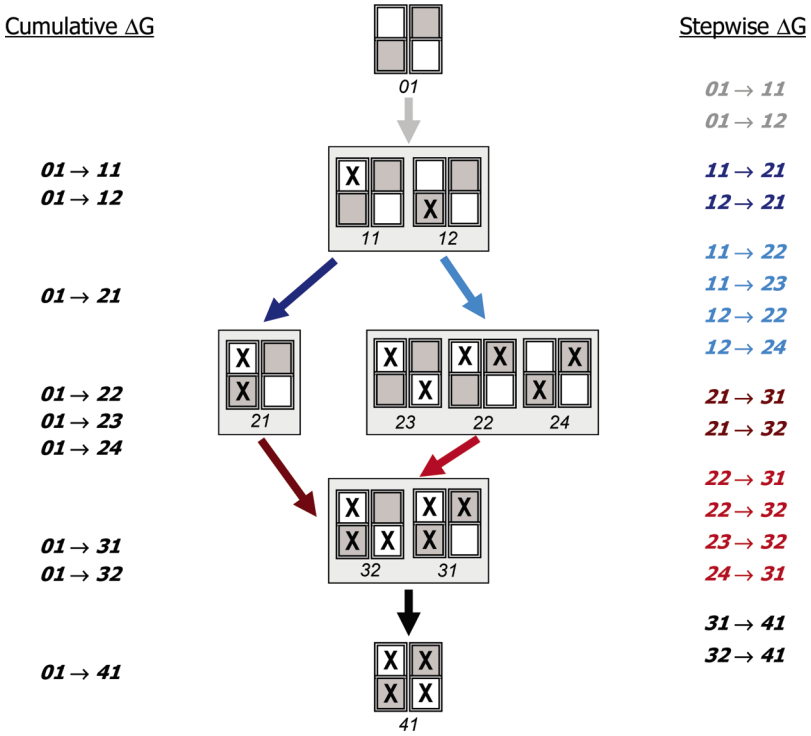

FIGURE 1: Asymmetric distribution of cooperativity in the Hb binding cascade. The cumulative and stepwise changes in free energy that comprise the O_2 binding cascade of human Hb. The Hb tetramer is illustrated with the β-subunits shaded, the O_2 ligand represented by X, and the ligand configurations designated as microstate species *ij*. The cascade is most commonly described by nine cumulative binding free energies, each of which is referenced to the deoxy (species ***01***) tetramer (listed at left), or equivalently, by 16 stepwise ΔG values, each of which consists of a single ligation step between specific binding configurations (listed at right). Both cumulative and stepwise changes in free energy can be transformed to the stoichiometric binding constants K_1, K_2, K_3, and K_4 to yield the sigmoidal O_2 binding curve.

it is shown that ligation of a deoxy dimer whose partner dimer is fully ligated occurs with low cooperativity. It is concluded that these low and noncooperative binding sequences are a general property of Hb under these solution conditions. The relationship of these results to previous observations made at the partially ligated stages in Hb is shown to be consistent with a dimer-based mechanism of cooperativity.

MATERIALS AND METHODS

Determination of Binding Free Energies from Assembly Free Energies

The experimental parameter for the hemesite analog systems which forms the basis for this analysis is the free energy of assembly of Hb tetramer from dimer, or ${}^{ij}\Delta G_2$. Assembly free energies are directly translated into ligand binding free energies via the thermodynamic linkage relationship between assembly and ligation, illustrated for binding two ligands (**X**) to a dimer in Hb:

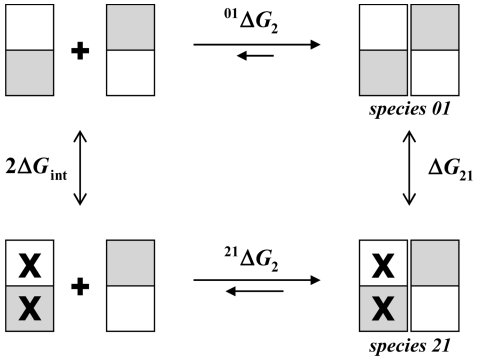

Ligation of the free dimer occurs with no cooperativity, providing an excellent thermodynamic reference state; binding to the free dimer is therefore defined as intrinsic binding, ΔG_{int}, for all hemesites. The binding free energy ΔG_{21} is not directly accessible experimentally, due to exchange of dimers among tetramers and O_2 ligand among hemesites which results in disproportionation to a solution of mixed species. But the assembly free energies can be measured accurately using a variety of techniques (i.e., the kinetic haptoglobin trapping method, large-zone size exclusion chromatography, sub-zero isoelectric focusing), while ligand exchange can be prevented through the use of stable hemesite analogs (as reviewed in ref 9). The change in assembly free energy is equal to the change in binding free energy, either of which yields the cooperative free energy ${}^{21}\Delta G_c$:

$$ {}^{21}\Delta G_2 - {}^{01}\Delta G_2 = \Delta G_{21} - 2\Delta G_{int} = {}^{21}\Delta G_c \qquad (1) $$

The tetrameric binding free energy is thus determined from two assembly free energies plus the intrinsic binding free energy:

$$ \Delta G_{21} = 2(\Delta G_{int}) + ({}^{21}\Delta G_2 - {}^{01}\Delta G_2) \quad \text{or} $$
$$ \Delta G_{21} = 2(\Delta G_{int}) + {}^{21}\Delta G_c \qquad (2) $$

Each binding step is therefore composed of an intrinsic ΔG, multiplied by the number of ligands bound, and a cooperative ΔG (Figure 2A**)**. When referenced to the deoxy tetramer, the cooperative free energy is, by definition, a cumulative free energy.

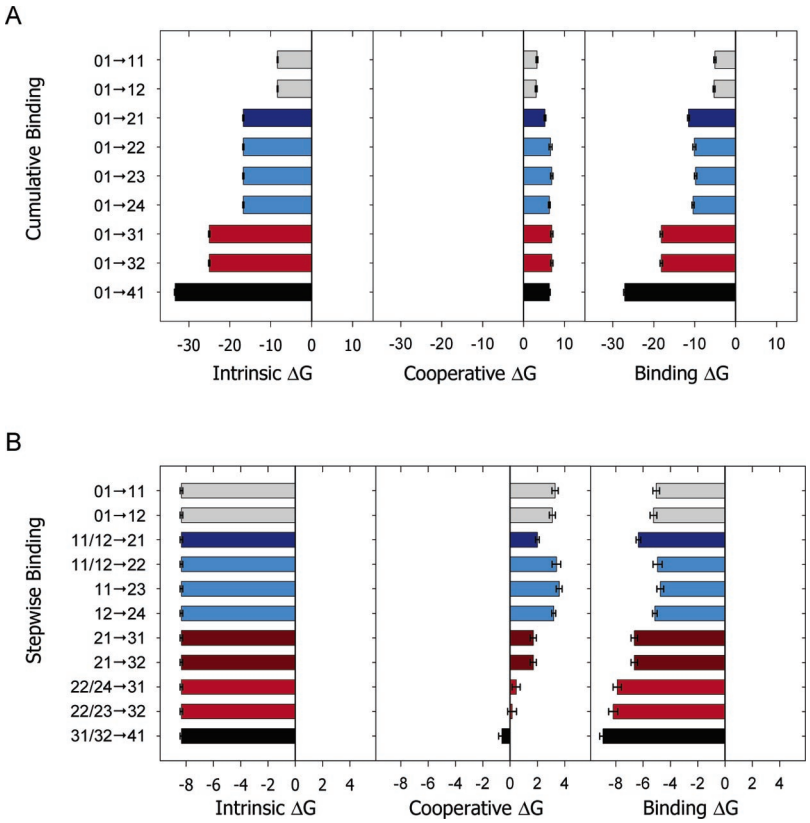

FIGURE 2: Energetic components of the binding free energy. Color coding of the bars is the same as in the cascade of Figure 1. (A) The nine cumulative binding steps are, by definition, referenced to the deoxy tetramer species ***01***. The intrinsic ΔG results from multiplying the intrinsic free energy of binding (−8.34 kcal/mol) by the total number of ligands bound. The free energy of ligand binding is equal to the intrinsic free energy plus the cooperative free energy: without the ΔG_c, binding to the tetramer would be noncooperative. (B) For stepwise binding, the intrinsic free energy is the same for each binding step. Of the 16 reactions, those with very similar binding energies have been grouped together, resulting in only 11 binding steps shown here. Cooperative ligand binding results from a stepwise decrease in the cooperative free energy penalty (shown in the middle panel), which is more readily observed in the stepwise reactions. Values for ${}^{ij}\Delta G_c$ were previously determined from measurements in a standard buffer of 0.1 M Tris, 0.1 M NaCl, 1 mM Na_2EDTA, pH 7.4, 21.5 °C. Errors were propagated as the square root of the sum of squares of the ${}^{ij}\Delta G_2$ experimental errors.

The intermediate binding constant k_{21} is related to ΔG_{21} by

$$k_{21} = \exp\left[\frac{-\Delta G_{21}}{RT}\right] \quad (3)$$

and is composed of both an intrinsic constant k_{int} and a cooperativity constant ${}^{21}k_c$:

$$k_{21} = (k_{int})^2({}^{21}k_c) \quad (4)$$

Error propagation for the conversion of ΔG_{ij} values to k_{ij} values was carried out by calculating k_{ij} from high and low values of ΔG_{ij}.

Both cooperative free energies and binding free energies can be expressed as stepwise values (Figure 1). The stepwise cooperative free energy for binding a ligand to species ***11*** to form species ***21*** is

$${}^{21}\Delta G_{cs} = {}^{21}\Delta G_2 - {}^{11}\Delta G_2 \quad (5)$$

where the subscript s denotes a stepwise free energy. As for cumulative values, each stepwise binding free energy ΔG_{ij} is composed of an intrinsic binding free energy and a cooperative free energy (Figure 2B). In the cumulative ΔG_{ij}, the intrinsic free energy is multiplied by the number of ligands bound, whereas each stepwise ΔG_{ij} includes a single ΔG_{int} value.

Cumulative Constants: Binding Isotherms for Complete Ligation

The nine microstate binding constants k_{ij} translate directly into the traditional O_2 binding curves in the following way. Contributions of all partially ligated intermediates to the overall binding isotherm of the Hb tetramer are contained within the binding polynomial Z_{tet},

$$Z_{tet} = 1 + K_1[O_2] + K_2[O_2]^2 + K_3[O_2]^3 + K_4[O_2]^4 \quad (6)$$

where K_i ($i = 1, ..., n$ and $n = 4$) are stoichiometric, or cumulative, binding constants, historically known as Adair constants (*2*). The fractional saturation of hemesites on a molar basis, $\bar{Y}$, is the derivative of the binding polynomial with respect to ligand concentration:

$$\bar{Y} = \frac{1}{n}\frac{d \ln Z_{tet}}{d \ln [O_2]} \quad (7)$$

Because it is a cumulative constant, each K_i is a weighted sum of binding constants for all the configurational isomers making up the cascade, k_{ij}, where j indexes the different configurations of bound ligand within a tetramer that has

bound *i* ligands, as in Figure 1. The composition of each K_i in terms of microstate binding constants is

$$K_1 = 2k_{11} + 2k_{12}$$
$$K_2 = 2k_{21} + 2k_{22} + k_{23} + k_{24}$$
$$K_3 = 2k_{31} + 2k_{32}$$
$$K_4 = k_{41} \quad (8)$$

Note that all K_i and k_{ij} are cumulative equilibrium constants where the uppercase denotes a macroconstant composed of the lowercase microconstants. The statistical factor of 2 applied to k_{11}, k_{12}, k_{21}, k_{22}, k_{31}, and k_{32} is required because these species can be formed in two structurally unique, but functionally indistinguishable, configurations (*2*), i.e., species ***11*** is either $\alpha_1[O_2]\beta_1{:}\alpha_2\beta_2$ or $\alpha_1\beta_1{:}\alpha_2[O_2]\beta_2$. For simplicity, the Hb cascade in Figure 1 shows only one of the two possible configurations for species ***11***, ***12***, ***21***, ***22***, ***31***, and ***32***.

The complete tetramer partition function, then, is

$$Z_{tet} = 1 + (2^{11}k_c + 2^{12}k_c)s + (2^{21}k_c + 2^{22}k_c + {}^{23}k_c + {}^{24}k_c)s^2 + (2^{31}k_c + 2^{32}k_c)s^3 + ({}^{41}k_c)s^4 \quad (9)$$

where $s = k_{int}[O_2]^i$. The binding isotherm is calculated directly from this partition function, in combination with eq 7,

$$\overline{Y} = \frac{({}^{1j}K_c)s + 2({}^{2j}K_c)s^2 + 3({}^{3j}K_c)s^3 + 4({}^{4j}K_c)s^4}{4\{1 + ({}^{1j}K_c)s + ({}^{2j}K_c)s^2 + ({}^{3j}K_c)s^3 + ({}^{4j}K_c)s^4\}} \quad (10)$$

where

$${}^{1j}K_c = 2^{11}k_c + 2^{12}k_c$$
$${}^{2j}K_c = 2^{21}k_c + 2^{22}k_c + {}^{23}k_c + {}^{24}k_c$$
$${}^{3j}K_c = 2^{31}k_c + 2^{32}k_c$$
$${}^{4j}K_c = {}^{41}k_c \quad (11)$$

Experimental error envelopes for $\overline{Y}$ were propagated from the ΔG_c error by calculating a lower limit isotherm using the upper limit values for all ${}^{ij}\Delta G_c$, and an upper limit isotherm using the lower limit values for all ${}^{ij}\Delta G_c$ terms.

Cumulative Constants: Binding Isotherms for Partial Ligation

The fractional saturation of hemesites developed above (eq 10) encompasses all binding configurations which contribute to the ligation of the deoxy tetramer (species ***01***). Subcascades, which also begin with species ***01***, but end with one of the partially ligated intermediates, may also be considered (Figure 3). For example, the binding curve from species ***01*** to the doubly ligated species ***21*** is described by

$$\overline{Y_{21}} = \frac{({}^{1j}K_c)s + 2({}^{2j}K_c)s^2}{2\{1 + ({}^{1j}K_c)s + ({}^{2j}K_c)s^2\}} \quad (12a)$$

where

$${}^{1j}K_c = {}^{11}k_c + {}^{12}k_c$$
$${}^{2j}K_c = {}^{21}k_c$$

Note that the statistical factor of 2, previously applied to the constants for species ***11***, ***12***, and ***21*** for complete ligation (eq 11), is no longer applicable. In the case of partial ligation to form species ***21***, one of the $\alpha\beta$ dimers within the tetramer must be considered to be "blocked", i.e., unavailable for binding. Thus, there is only one configuration of species ***21*** formed, and likewise only one configuration of species ***11*** and ***12*** in the species ***21*** subcascade.

The remaining subcascades are developed similarly.

species ***22***: $$\overline{Y_{22}} = \frac{({}^{11}k_c + {}^{12}k_c)s + 2({}^{22}k_c)s^2}{2\{1 + ({}^{11}k_c + {}^{12}k_c)s + ({}^{22}k_c)s^2\}} \quad (12b)$$

species ***23***: $$\overline{Y_{23}} = \frac{(2^{11}k_c)s + 2({}^{23}k_c)s^2}{2\{1 + (2^{11}k_c)s + ({}^{23}k_c)s^2\}} \quad (12c)$$

species ***24***: $$\overline{Y_{24}} = \frac{(2^{12}k_c)s + 2({}^{24}k_c)s^2}{2\{1 + (2^{12}k_c)s + ({}^{24}k_c)s^2\}} \quad (12d)$$

species ***31***:

$$\overline{Y_{31}} = \frac{(2^{11}k_c + 2^{12}k_c)s + 2({}^{21}k_c + {}^{22}k_c + {}^{24}k_c)s^2 + 3({}^{31}k_c)s^3}{3\{1 + (2^{11}k_c + 2^{12}k_c)s + ({}^{21}k_c + {}^{22}k_c + {}^{24}k_c)s^2 + ({}^{31}k_c)s^3\}} \quad (12e)$$

for species ***32***:

$$\overline{Y_{32}} = \frac{(2^{11}k_c + {}^{12}k_c)s + 2({}^{21}k_c + {}^{22}k_c + {}^{23}k_c)s^2 + 3({}^{32}k_c)s^3}{3\{1 + (2^{11}k_c + {}^{12}k_c)s + ({}^{21}k_c + {}^{22}k_c + {}^{23}k_c)s^2 + ({}^{32}k_c)s^3\}} \quad (12f)$$

Note that, in the case of the species ***23*** subcascade, both α-subunits are available for binding; therefore the statistical factor for species ***11*** is 2. This is also the case for species ***11*** in the ***32*** subcascade, and for species ***12*** in the ***24*** and ***31*** subcascades.

The tetrameric binding curves were determined for a range of hemesite analogs for which direct ligand binding measurements are either not possible or not practical, and therefore no value for the intrinsic binding constant, k_{int}, exists. The analog binding curves were therefore normalized by employing the normal Hb k_{int}.

Cumulative Constants: The Hill Coefficient

The Hill coefficient, ${}^{ij}n_H$, is derived from the dependence of fractional saturation, $\overline{Y_{ij}}$, on ligand concentration for binding to form the *ij* intermediate:

$${}^{ij}n_H = \frac{d \ln\left(\frac{\overline{Y_{ij}}}{1 - \overline{Y_{ij}}}\right)}{d \ln [O_2]} \quad (13)$$

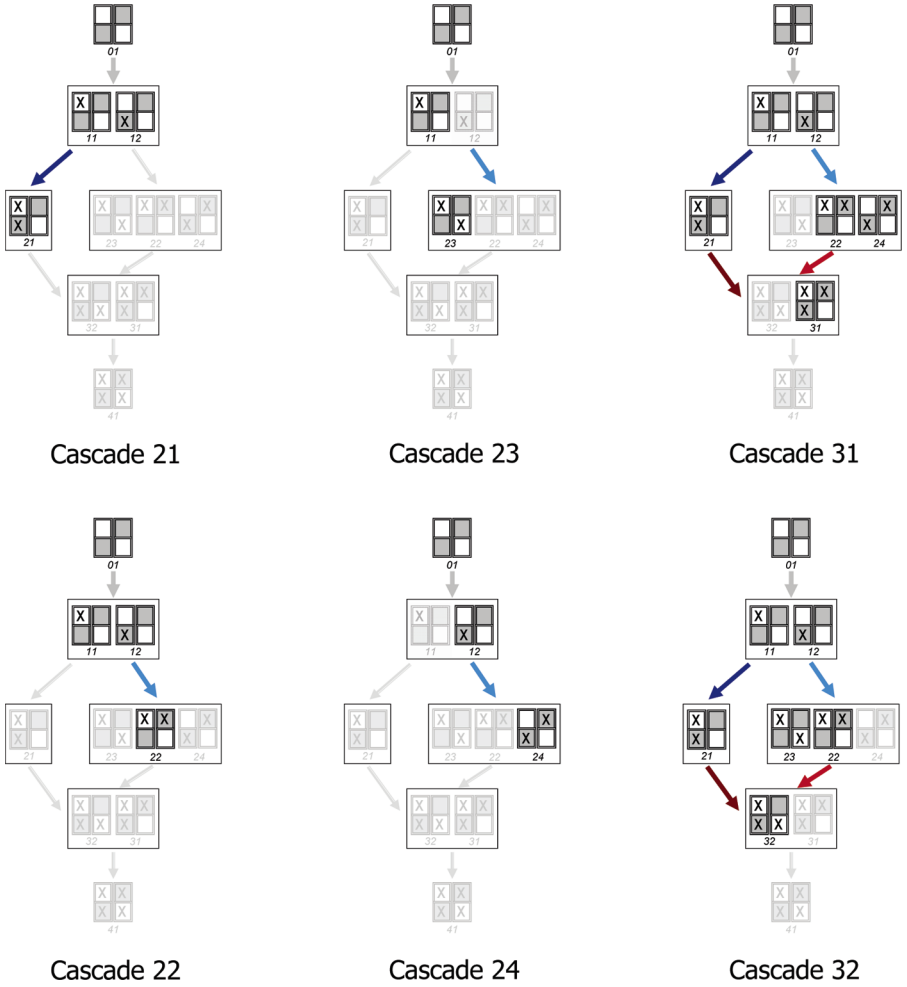

FIGURE 3: Partially ligated Hb binding cascades. Each binding reaction that contributes to the isotherm for each species (shown in Figure 4) is highlighted. Thus, for example, both species ***11*** and ***12*** contribute to the binding curve of species ***21***, while only species ***11*** contributes to the binding curve of species ***23***.

Although the value of the Hill coefficient is dependent upon ligand concentration (via $\overline{Y_{ij}}$), it is generally reported as a single n_H value corresponding to the maximum slope of eq 13 over the complete binding process. In the present study, the Hill coefficient is related to the standard deviation of $\overline{Y_{ij}}$,

$$ {}^{ij}n_H = \frac{\overline{Y_{ij}^2} - 4(\overline{Y_{ij}})^2}{\overline{Y_{ij}}(1 - \overline{Y_{ij}})} \qquad (14)$$

in that the difference between the mean square value $\overline{Y_{ij}^2}$ and the square of the mean value $(\overline{Y_{ij}})^2$ is the standard deviation of $\overline{Y_{ij}}$, as previously shown by Edsall (*10*, *11*) and Wyman (*12*) (see Discussion). Error propagation for ${}^{ij}n_H$ was carried out here in the same manner as described for the error envelope of $\overline{Y_{ij}}$.

RESULTS

Hb cooperativity was assessed in terms of both intensive or cumulative (Hill coefficient, n_H) and extensive or stepwise (${}^{ij}\Delta G_c$) parameters for nine Hb systems. The distribution of binding free energy was found to follow a consensus pattern among all those Hbs, in agreement with that previously observed for the cumulative free energies (*1*−*3*).

Cooperativity Measured by Cumulative Free Energies

The cooperative free energy for all 16 steps comprising the cascade, ${}^{ij}\Delta G_c$, has been reported for all *ij* microstate configurations in a variety of Hbs carrying hemesite analog substitutions (Table 1). For Hb tetramers whose native deoxy Fe^{2+}- or ligated FeO_2-hemes have been substituted with hemesite analogs, the cumulative cooperative free energy ranges from $+7.4 \pm 0.4$ kcal/mol (Mg^{2+} substitution for deoxy Fe^{2+}) to only $+2.3 \pm 0.1$ kcal/mol (Co^{2+} substitution for deoxy Fe^{2+} or $Fe^{3+}CN$ substitution for $Fe^{2+}O_2$), as compared to $+6.3 \pm 0.1$ kcal/mol for native Hb. In spite of the variations induced by analog substitution, the distribution of the cumulative ${}^{ij}\Delta G_c$ as well as the stepwise ${}^{ij}\Delta G_{cs}$ in the binding cascade follows a *consensus pattern* (*1*, *3*, *6*):

$$({}^{11}\Delta G_{cs} \approx {}^{12}\Delta G_{cs}) < {}^{21}\Delta G_{cs} < ({}^{22}\Delta G_{cs} \approx {}^{23}\Delta G_{cs} \approx {}^{24}\Delta G_{cs} \approx {}^{31}\Delta G_{cs} \approx {}^{32}\Delta G_{cs}) < {}^{41}\Delta G_{cs} \qquad (15)$$

Isotherms for Hb Analogs. Of the Hb species for which data is available for this study, direct oxygen binding measurements have only been reported for native Hb (the Adair constants) (*13*, *16*) and species ***23*** and ***24*** of Zn/FeO_2 (*7*, *8*, *17*). The Zn/FeO_2 isotherms show behavior very similar to that of the Adair binding curves, in that the doubly ligated

Table 1: Cumulative Cooperative Free Energies for Hb Analogs in All Possible Configurations of Bound Ligand in Wild-Type Tetramers[a]

hemesite analogs unligated:ligated	cooperative free energies, $^{ij}\Delta G_c$, kcal/mol									
	species ***11***	species ***12***	species ***21***	species ***22***	species ***23***	species ***24***	species ***31***	species ***32***	species ***41***	ref
Fe^{2+}: FeO_2	2.9 ± 0.2		5.7 ± 1.3				7.1 ± 1.7		6.3 ± 0.1	*13*
Zn^{2+}:FeO_2	3.4 ± 0.1	3.1 ± 0.1	5.2 ± 0.1	6.6 ± 0.4	6.9 ± 0.2	6.3 ± 0.1	6.9 ± 0.3	6.9 ± 0.3	6.3 ± 0.2	*7*
Mg^{2+}:FeO_2	3.3 ± 0.5	3.4 ± 0.6	(5.7 ± 0.6)	7.0 ± 0.6	7.4 ± 0.4	6.5 ± 0.4	7.9 ± 0.5	8.2 ± 0.5	7.4 ± 0.4	*14*
Co^{2+}:FeCO	1.6 ± 0.2	2.2 ± 0.2	2.3 ± 0.2	3.2 ± 0.2	3.1 ± 0.2	3.2 ± 0.2	2.9 ± 0.2	3.0 ± 0.2	2.6 ± 0.1	*15*
Mg^{2+}:FeCO	3.8 ± 0.5	3.5 ± 0.6	(5.7 ± 0.6)	8.4 ± 1.1	7.8 ± 0.5	7.7 ± 0.5	7.8 ± 0.6	7.7 ± 0.6	7.4 ± 0.4	*14*
Fe^{2+}:FeCO	3.3 ± 0.3	3.4 ± 0.4	(5.2 ± 0.4)	6.5 ± 0.4	6.6 ± 0.4	6.5 ± 0.4	6.5 ± 0.4	6.6 ± 0.4	6.4 ± 0.2	*15*
Fe^{2+}: Fe^{3+}CN	3.1 ± 0.3	3.3 ± 0.3	4.3 ± 0.3	6.4 ± 0.3	6.1 ± 0.3	6.4 ± 0.3	6.3 ± 0.3	6.2 ± 0.3	6.1 ± 0.2	*1, 15*
Co^{2+}:Fe^{3+}CN	1.7 ± 0.1	2.1 ± 0.1	(3.2 ± 0.4)	3.1 ± 0.1	2.9 ± 0.1	3.1 ± 0.1	2.9 ± 0.1	2.7 ± 0.2	2.3 ± 0.1	*15*
Fe^{2+}:Mn^{3+}	2.9 ± 0.4	3.7 ± 0.4	(4.6 ± 0.4)	6.6 ± 0.4	6.8 ± 0.4	6.2 ± 0.4	6.5 ± 0.4	6.5 ± 0.4	6.9 ± 0.4	3

[a] Solution conditions for all studies were 21.5 °C, pH 7.4, 0.1 M Tris, 0.1 M NaCl, 1 mM Na_2EDTA (total chloride 0.18 M). Parentheses indicate values estimated as the average of parent assembly free energies plus 2 kcal (see text).

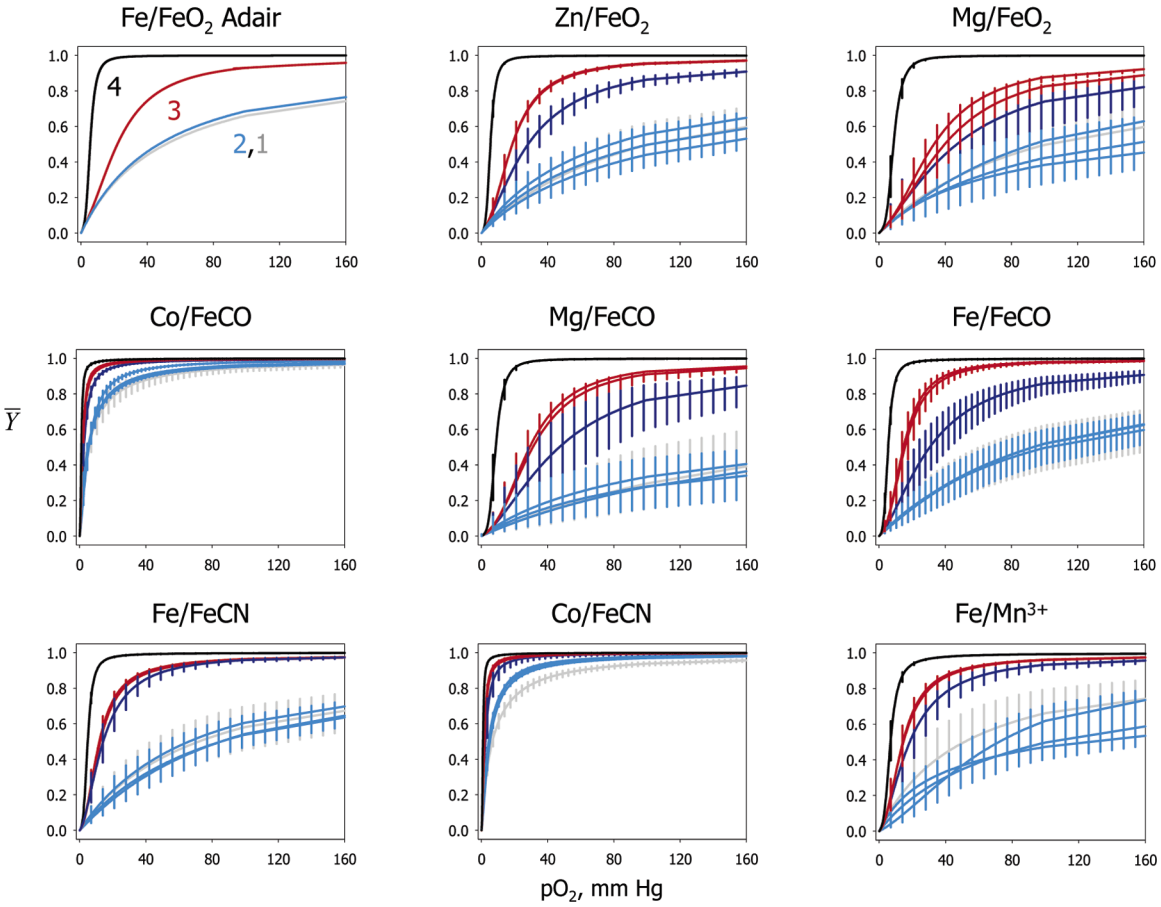

FIGURE 4: Calculated binding curves for each partially ligated Hb microstate up to the partial pressure of O_2 in air. The binding curves are determined from the cumulative cooperative free energies and their corresponding uncertainties (Table 1) and are color-coded according to the corresponding subcascade (Figure 3). Very large experimental errors in the second and third binding steps in the native Hb curves (designated as Adair) have been omitted for clarity.

species ***22***, ***23***, and ***24*** bind incompletely under atmospheric O_2 pressure (*7*). Isotherms for non-oxygen ligands were calculated using the intrinsic O_2 binding constant (Figure 4). Incomplete ligation at 160 mmHg is observed in species ***22***, ***23***, and ***24***, ranging from ~30% saturation in Mg/FeCO to ~95% saturation in the high-affinity Co/FeCO and Co/FeCN Hb analogs.

The Maximum Hill Coefficient, n_H. In comparing maximum Hill coefficients between the different subcascades, it should be noted that the increase in Hill coefficient with increasing number of ligands bound cannot be interpreted in terms of increasing cooperativity (Figure 5). The largest possible Hill coefficient for a doubly ligated cascade is two, i.e., the case in which cooperativity is infinite. Likewise, the largest possible n_H for the ***31*** or ***32*** cascade is three, and for the complete cascade is four.

Binding to form species ***21*** yields a maximum n_H significantly greater than one in all analog Hbs. In contrast, ligand binding to form species ***22***, ***23***, and ***24*** is typically noncooperative. The exception may be found in the two analogs in which Co^{2+} heme is substituted for deoxy Fe^{2+} heme, where positive cooperativity is observed, particularly in species ***24***. The tendency toward negative cooperativity in both Zn/FeO_2, Mg, and Fe/Mn^{3+} analogs does not appear to be significant within the limits of error propagated from the $^{ij}\Delta G_c$ values.

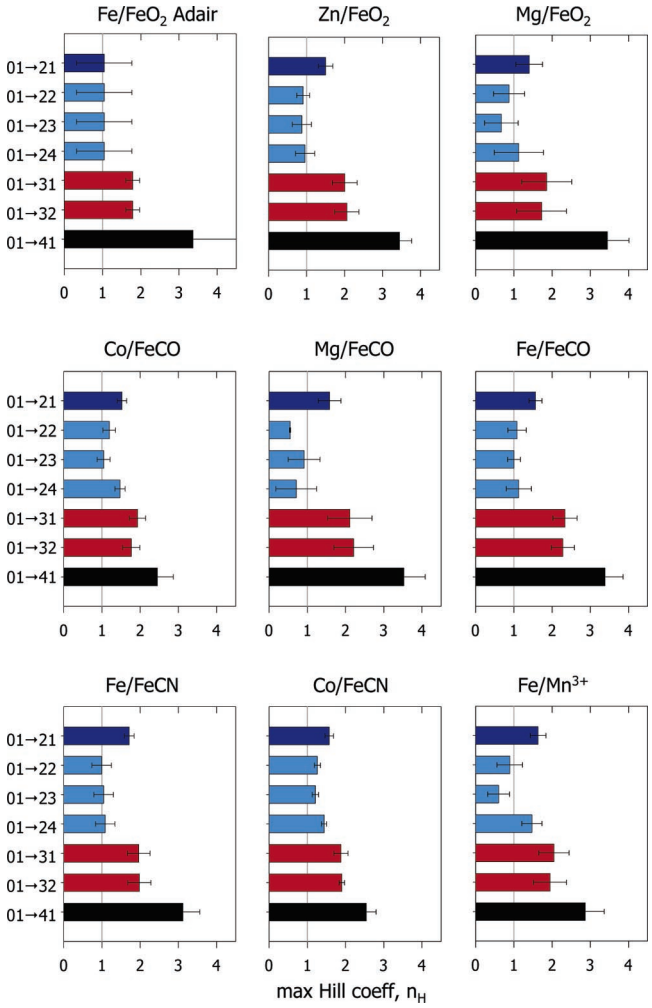

FIGURE 5: Maximum Hill coefficients corresponding to the binding isotherms for each partially ligated Hb microstate shown in Figure 4. Noncooperative binding is indicated by a value of one. The largest possible value for the Hill coefficients increases with the number of ligands bound.

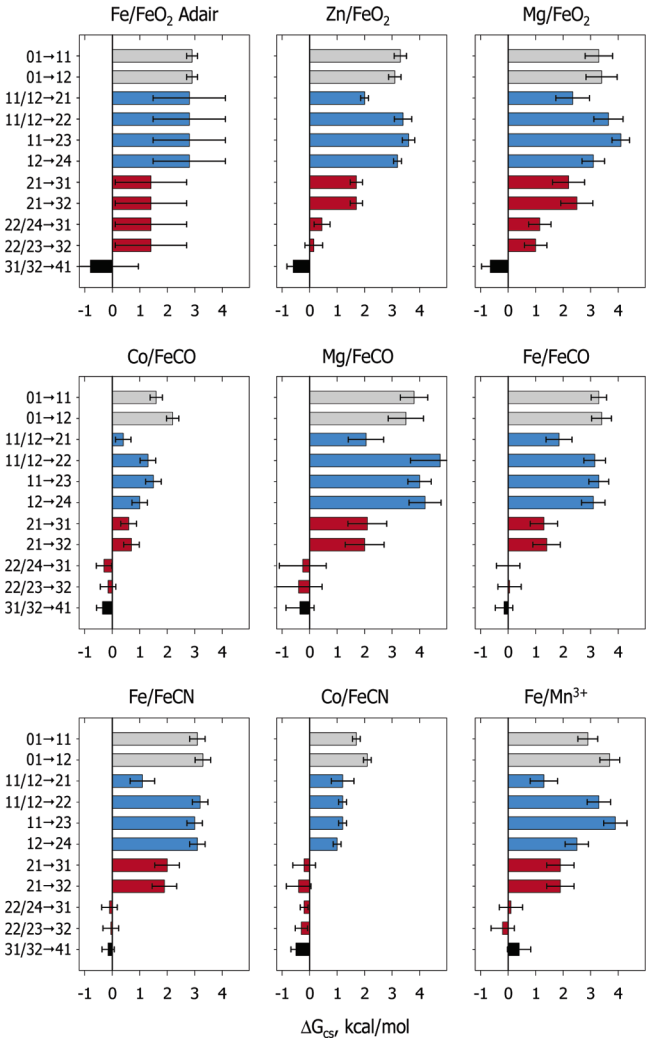

FIGURE 6: Stepwise cooperative free energies for all 16 binding reactions in the Hb cascade. Reactions found to be energetically redundant are grouped for clarity. All analogs for which the ${}^{ij}\Delta G_c$ value can be assessed for each intermediate are included in this analysis, and all data was collected at 21.5 °C, pH 7.4.

Cooperativity Measured by Stepwise Free Energies

The distribution of the stepwise ${}^{ij}\Delta G_{cs}$ in the binding cascade (Figure 6) follows a *consensus pattern* among Hb analogs:

$$({}^{01\rightarrow11}\Delta G_{cs} \approx {}^{01\rightarrow12}\Delta G_{cs}) \approx ({}^{11/12\rightarrow22}\Delta G_{cs} \approx {}^{11\rightarrow23}\Delta G_{cs} \approx {}^{12\rightarrow24}\Delta G_{cs}) > {}^{11/12\rightarrow21}\Delta G_{cs} \approx ({}^{21\rightarrow31}\Delta G_{cs} \approx {}^{21\rightarrow32}\Delta G_{cs}) > ({}^{22/24\rightarrow31}\Delta G_{cs} \approx {}^{22/23\rightarrow32}\Delta G_{cs}) > {}^{31/32\rightarrow41}\Delta G_{cs} \quad (16)$$

*Noncooperativity in Species **22**, **23**, and **24***. The absence of cooperativity in the binding of the first two ligands, one ligand to each dimer, occurs when the stepwise ${}^{ij}\Delta G_c$ is the same for the first and second binding steps. This condition is met within the range of experimental error for the majority of all analogs studied to date (Figure 6). Positive cooperativity is observed in those cases where Co^{2+}-heme is used as an analog for deoxy Fe^{2+}, i.e., in Co/FeCO and Co/FeCN. In these analog microstates, the stepwise cooperative free energy for species ***22***, ***23***, and ***24*** is generally less than that for species ***11*** and ***12***. A slight negative cooperativity in species ***22***, ***23***, and ***24*** is suggested in the cases where Mg^{2+} is employed as a deoxy hemesite analog: Mg/FeO_2 and Mg/FeCO and, to a lesser extent, in Zn/FeO_2 and Fe/Mn^{3+}. However, the propagated errors are large enough to prevent a clear assignment of negative cooperativity in each case. For these and the remaining analogs, binding to form species ***22***, ***23***, and ***24*** is therefore concluded to be noncooperative within the error of the measurements.

For comparison with traditional O_2 binding experiments to native Fe/FeO_2 Hb, the four Adair binding constants were partitioned into ${}^{ij}\Delta G_{cs}$ values by setting the microstate ${}^{ij}\Delta G_{cs}$ values for native Hb equal to one another at each *i* binding step, i.e., that for species ***21*** is equal to the other doubly ligated species because it cannot be resolved by the Adair constants (Figure 4). The large propagated errors for the second, third, and fourth binding steps (Figure 6) arise from the large experimental errors for K_2 and K_3 (*2*, *13*). Due to this large uncertainty, a definitive conclusion of cooperativity in many of the intermediate binding sequences cannot be made: it can only be concluded that there is no discrepancy between the microstate constants from substituted Hbs and the Adair constants from native Hb.

*Positive Cooperativity in Species **21***. In contrast to species ***22***, ***23***, and ***24***, binding to form species ***21*** occurs with

positive cooperativity, which is observed as a smaller $^{ij}\Delta G_{cs}$ for species ***21*** relative to that for the first binding steps (to form species ***11*** or ***12***) (Figure 6). Only in the cases of Mg/FeO_2 and Co/FeCN is there overlap of the propagated errors among species ***21***, ***11***, and ***12***. In the case of the Adair constants, species ***21*** is part of an average which includes the other doubly ligated species.

*Positive Cooperativity and Noncooperativity in Species **31** and **32***. Binding the third ligand to species ***22***, ***23***, or ***24*** to form species ***31*** or ***32*** carries a small $^{ij}\Delta G_{cs}$ in each analog, indicative of large positive cooperativity (Figure 6). In contrast, the propagated errors for binding the third ligand to species ***21*** to form species ***31*** or ***32*** are overlapping, with the exception of Co/FeCN. Due to this uncertainty, there is no compelling evidence for large positive cooperativity in binding the third ligand to species ***21***, (e.g. ***11*** or ***12*** → ***21*** → ***31*** or ***32***), although there appears to be a trend to a small degree of positive cooperativity. This is in contrast to the very distinct difference in ΔG_{cs} between species ***22***, ***23***, and ***24*** and species ***31*** and ***32***, indicative of large cooperativity in every analog system.

Positive Cooperativity in the Fourth Binding Step. Binding the fourth ligand either to species ***31*** or ***32*** to form species ***41*** typically exhibits a negative $^{ij}\Delta G_{cs}$, e.g., the final binding step to the tetramer typically occurs with a higher affinity than that of the free dimer. This phenomenon, known as quaternary enhancement, is experimentally observed in both microstate analogs and native Hb (*16*, *18*−*21*). In some analogs, quaternary enhancement is evident at the third binding step as well.

DISCUSSION

The distribution of cooperative free energy among the Hb microstate intermediates is key to understanding the sequence through which the subunits within the tetramer communicate. Over the past decade, work on the Hb microstates has revealed that cooperativity is manifested in both intradimer and cross-dimer interactions within the tetramer, which represents a significant departure from the concerted, two-state view that dominated several decades of Hb research (*2*, *6*).

In order to evaluate the contribution to cooperativity by each of the sixteen ligation steps that comprise the Hb cascade, it has been necessary to use nonlabile hemesite analogs to fix the arrangement of ligands among the α- and β-subunits of the tetramer. This approach also requires the use of linkage thermodynamics to determine binding free energies of the intermediate ligation steps, since most hemesite analogs do not lend themselves to direct binding measurements. An exception to this rule is the use of Zn^{2+} heme as a deoxy heme analog, which permits the measurement of direct O_2 binding to native Fe hemesites in Zn/Fe hybrid tetramers. Even when O_2 exchange among hemesites is controlled in this way, direct O_2 binding studies are still limited to the symmetric tetramers, species ***23*** and ***24***, due to dimer exchange that results in disproportionation of asymmetric hybrids during the course of O_2 binding.

As shown in the previous report (*7*), O_2 binding to form species ***23*** and ***24*** of the Zn-substituted Hb is incomplete and noncooperative. These characteristics are not typically associated with the behavior of normal human Hb, and it is initially compelling to assign these observations to an artifact of Zn-heme substitution (*17*). And yet, incomplete, noncooperative binding at the second binding step is predicted by the Adair constants, measured using traditional experimental methods with normal, unmodified Hb. In addition, as demonstrated in the present study, noncooperative binding in species ***22***, ***23***, and ***24*** is not limited to Zn-substituted Hb, but is a general feature observed over a range of hemesite analog subsitutions. Taken together, these data indicate that binding the first two ligands, one ligand per dimer, occurs with no significant cooperativity in normal human Hb under the conditions of these studies. In contrast, binding the first two ligands on the same dimer exhibits strong positive intradimer cooperativity. Thus, cooperativity is distributed asymmetrically within the Hb binding cascade.

The noncooperative sequence of binding two ligands to form species ***22***, ***23***, or ***24*** involves binding a ligand onto a deoxy dimer whose partner dimer is already ligated. This binding scenario also occurs upon binding the third ligand to species ***21***, from species ***11*** or ***12*** to species ***21*** to species ***31*** or ***32***, a two-step binding sequence which also exhibits little or no positive cooperativity. Unlike the first two binding steps, in which the noncooperative nature of the binding sequence is clear from both cumulative or stepwise binding free energies, the species ***21*** binding sequence is only observable using the stepwise cooperative free energies. The possible significance of the lack of positive cooperativity in binding to a deoxy dimer when the partner dimer is already ligated is discussed further below.

Cooperative Free Energy vs the Hill Coefficient

Each of the O_2 binding steps in any given pathway through the Hb cascade includes an intrinsic free energy of binding. As the deoxy Hb tetramer binds O_2 with much lower affinity than the deoxy free dimer, an energetic penalty or cooperative free energy, $^{ij}\Delta G_c$, has been applied to the tetramer. Each additional O_2 binds to the tetramer with a smaller energetic penalty until, at the fourth binding step, the tetramer binding affinity is actually greater than that of the free dimer. Although $^{ij}\Delta G_c$ is typically reported as a cumulative value (for binding i ligands in configuration j to the deoxy tetramer), the development of cooperativity within the cascade is best evaluated by the incremental or stepwise $^{ij}\Delta G_{cs}$ values, i.e., the free energy change for binding a single ligand. The stepwise cooperative free energy is thus a fundamental value which cannot be further partitioned.

All combinations of the microstate k_{ij} values which sum to the same four K_i values (the four Adair constants) will specify an identical binding curve. In principle, then, for any set of four Adair constants there is no unique set of microstate binding constants that can be deduced without additional experimental data (*2*). Thus, while numerical analysis of a measured $\bar{Y}$ vs [free ligand] data set can resolve the four best fit K_i Adair constants, such fitting cannot provide unique values of the nine constituent microconstants k_{ij}, regardless of the accuracy of experimental data or statistical confidence limits of parameter estimates. This limitation applies to other functions that depend solely on $\bar{Y}$, including the Hill coefficient n_H and other parameters derived from the higher statistical moments of the $\bar{Y}$ function.

The Hill coefficient therefore differs fundamentally from the stepwise cooperative free energy in that n_H represents a

measure of statistical variance of the binding constant among the microstates (*11*). The relationship of n_H to the variance was pointed out by Edsall (*10*) and further developed by Wyman (*12*) based upon the following derivation attributed to Linderström-Lang (for $d\bar{v}/d(\ln [H^+]) = -d\bar{v}/d(pH)$) for the proton binding curves of proteins and polyelectrolytes in general (*10*, *12*). From the Hill equation,

$$n_H = \frac{d \ln \frac{\overline{Y}}{n - \overline{Y}}}{d \ln [O_2]} \tag{17}$$

where n is the number of binding sites,

$$\begin{aligned} n_H &= \frac{n}{\overline{Y}(n - \overline{Y})} \frac{d\overline{Y}}{d \ln [O_2]} \\ &= \frac{n}{\overline{Y}(n - \overline{Y})} \frac{d}{d \ln [O_2]} \frac{\sum i\overline{K_i}[O_2]^i}{\sum_{i=0}^{n} \overline{K_i}[O_2]^i} \\ &= \frac{n}{\overline{Y}(n - \overline{Y})} \left\{ \frac{\sum i^2 \overline{K_i}[O_2]^i}{\sum \overline{K_i}[O_2]^i} - \left(\frac{\sum i\overline{K_i}[O_2]^i}{\sum \overline{K_i}[O_2]^i} \right)^2 \right\} \\ &= \frac{n}{\overline{Y}(n - \overline{Y})} \{\overline{Y^2} - (\overline{Y})^2\} \end{aligned} \tag{18}$$

where i is the number of ligands bound. The expression $\overline{Y^2} - (\overline{Y})^2$ is proportional to the standard deviation of the distribution of bound ligand. Thus, the higher the Hill coefficient, the more nonrandom the distribution of binding constants over the range of oxygen concentration. Cooperativity generates a change in the binding constant, increasing the variance. Factors other than cooperativity can cause dispersion of binding constants, the most notable being different intrinsic binding between α- and β-subunits (which manifests as apparent negative cooperativity). Because it represents a statistical distribution, the Hill coefficient can also mask microstate distributions in favor of the overall variance. Thus, a large value of n_H can be associated with the binding cascade of Hb without revealing that some of the binding sequences are noncooperative. Still, the Hill coefficient is useful as a measure of cooperativity, and when limited to a two-step binding process, it can be quite specific.

The relative effectiveness of the stepwise cooperative free energy and the Hill coefficient in analyzing a cooperative cascade such as found in human Hb is illustrated in the present analysis. In the first two binding steps, from deoxy species ***01*** to species ***21***, ***22***, ***23***, or ***24***, the two parameters both indicate positive cooperativity in species ***21*** and noncooperativity in species ***22***, ***23***, and ***24***. When the third binding step is included, the Hill coefficient reports large positive cooperativity, hiding the almost noncooperative sequence from species ***11*** or ***12*** to species ***31*** or ***32*** through species ***21*** that is readily observed in the stepwise cooperative free energies.

Noncooperativity and Dimer Autonomy in Hb

Analysis of the free energies associated with ligand binding has been carried out and presented in this study in a model-independent manner. The significance of these findings to allosteric models is now considered. The consensus distribution of microstate cooperative free energies among the eight ligation intermediates of Hb is fundamentally incompatible with a two-state energetic model of cooperativity (*1*−*3*). The limitation of only two energetic states of the tetramer (high and low affinity) dictates that the energetic contributions to cooperativity from the intermediate ligation states be additive. The cooperative free energies of the microstates are not found to be additive, however, whether in native or asymmetrically modified tetramers (*6*). In 1992, the symmetry rule model was introduced to provide a structural basis for the cooperative free energy distribution among the microstates (Figure 7). In this model, the deoxy tetramer remains in a T quaternary structure until at least one ligand is bound to each dimer. The T structure is defined in terms of the orientation of the two dimers relative to one another. Ligands on both dimers, in any site configuration, result in a quaternary switch to the R structure, i.e., a change in the dimer−dimer orientation. The cooperative free energy for ligation within the T class of microstates is therefore tertiary (or intradimer) in nature, referred to as the free energy of tertiary constraint. The symmetry rule model posits six ligation-induced quaternary switchpoints: from species ***11*** to either ***22*** or ***23***; from species ***12*** to either ***22*** or ***24***; and from species ***21*** to either ***31*** or ***32***. In these switchpoint steps, the tertiary constraint from ligation in the T structure is released, helping to pay for the energetically expensive T → R conversion (*2*, *22*). In this sense, the formation and release of tertiary constraint is viewed as a fundamental driving force of Hb cooperativity in the symmetry rule model.

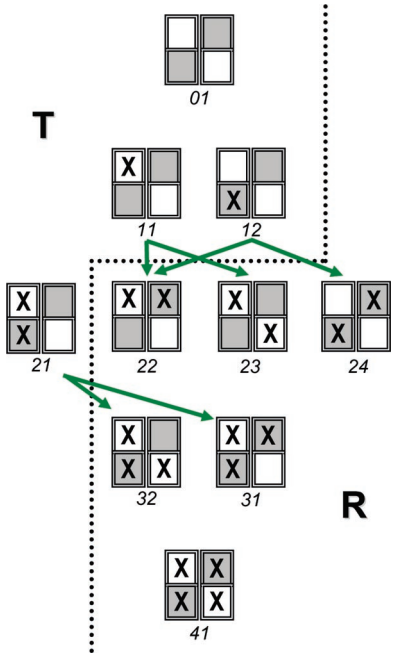

FIGURE 7: The six quaternary switchpoints in the symmetry rule model. The first oxygen binding step to the deoxy tetramer (species ***01***) is communicated to the other subunit within the αβ dimer. When at least one subunit in each dimer is oxygenated, the resulting tertiary changes disfavor the T interface and promote quaternary switching to the R interface. In this model, most of the binding cooperativity results from the quaternary switch, which itself is controlled by the six switchpoint binding steps: from species ***11*** to ***22*** or ***23***; from species ***12*** to ***22*** or ***24***; and from species ***21*** to ***31*** or ***32***.

The net cooperative free energy change upon binding all four O_2 ligands to Hb is +6.3 kcal/mol under the conditions of these studies. The symmetry rule model places the majority of the net cooperative free energy change in the dimer−dimer interface bonds, that is, the model charges 6.3 kcal/mol of free energy to break the T structure dimer−dimer bonds, rotate the dimers, and form the R structure interface bonds (including solvent rearrangement). The basis of this assignment of cooperative free energy is the widely accepted tenet that the low affinity of the T structure is due to the constraint placed on its hemesites by the bonds of the dimer−dimer interface. In the high-affinity R structure, the interface is weakened, releasing the constraint on the hemesites. In this case, the symmetry rule model and the historical two-state model are based on the same assumption.

A classic Hb experiment places a mutation or chemical modification in the dimer−dimer interface, removing or weakening T structure contacts, and invariably resulting in a much higher affinity tetramer (as discussed in ref *6*). In the example of desArg Hb, the C-terminal Arg of the α-subunits is removed enzymatically, eliminating $\alpha^1-\alpha^2$ salt bridge contacts in the deoxyHb dimer−dimer interface, as confirmed by crystallography (*23*). The modification results in a high affinity tetramer. As is the case for essentially all human Hb mutants, both dimers within the tetramer carry the modification. When the Arg was removed from only a single α-subunit, forming a hybrid tetramer consisting of a desArg dimer and a wild-type dimer, ligation to the wild-type dimer exhibited a wild-type ${}^{ij}\Delta G_c$, while ligation to the desArg dimer yielded a ${}^{ij}\Delta G_c$ reduced by 2 kcal/mol (a third of the overall cooperative free energy of ligation in Hb), resulting in high ligand affinity (*6*). This asymmetric modification, and others applied throughout the dimer−dimer interface, demonstrated an autonomous response of the dimers within the tetramers that could not be identified when both dimers carried the same perturbation.

The results of the asymmetric modification and asymmetric ligation studies cast significant doubt on a fundamental premise of the symmetry rule model and the historical two-state model: that the great majority of the net cooperative free energy change in Hb is due to the T → R quaternary switch. Interestingly, the low, or noncooperative, binding steps identified in the present study are the same six quaternary switchpoint ligation steps of the symmetry rule model. These findings require additional formulation of the model, which falls outside the focus of the present study. But the following caveats can be made with respect to the mechanistic significance of noncooperative binding sequences. First, noncooperativity in a binding sequence simply means that no significant change has been measured in a free energy parameter (ΔG_c, ΔG_2, ΔG_i) from one reaction to the next. But the two binding events may likely result from different structural properties. In general, where a free energy change is observed, a structural change has also occurred (either in solute or solvent or both), but in the absence of change in free energy, no definitive conclusion can be reached as to whether a structural change has, or has not, occurred. In this sense, then, the low cooperativity or noncooperativity of two sequential binding steps in the Hb cascade should not be attributed, from these data alone, to an autonomous response of the dimers within the tetramer.

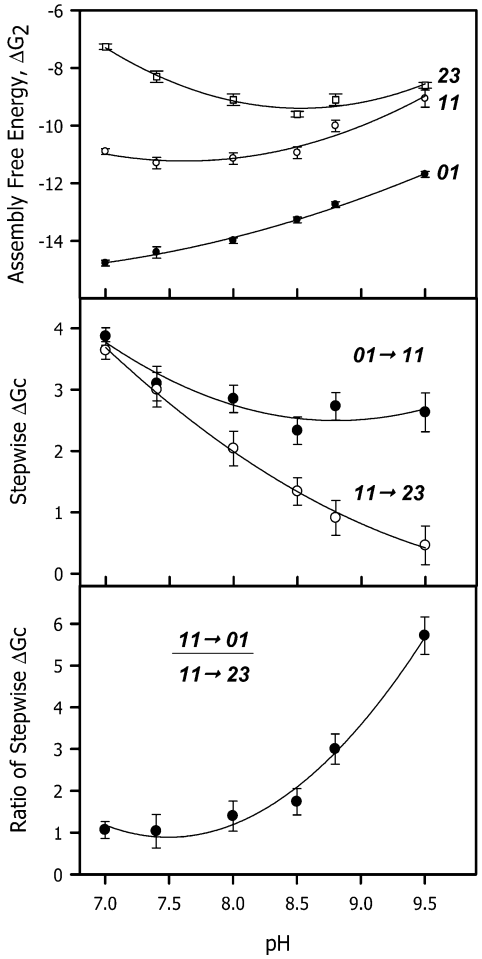

FIGURE 8: Dependence of cooperativity in species ***23*** on pH. The assembly free energies for species ***01***, ***11***, and ***23*** were measured with respect to pH for the Fe/FeCN analog system (*24*) (upper panel). The stepwise cooperative free energies are determined by subtraction (middle panel). At neutral pH, the noncooperative nature of the binding sequence is observed as 1:1 ratio of the stepwise ΔG_c of the two binding steps. The ratio increases significantly beyond unity as the pH increases, indicative of positive cooperativity.

Second, the presence of low or no cooperativity in certain binding sequences does not appear to be an artifact of hemesite substitution; however, this does not mean that it is present in vivo either. For example, in the Fe^{2+}/Fe^{3+}CN analog system, in which the stepwise cooperative free energies have been measured over the alkaline pH range (*24*), positive cooperativity in the ***01*** → ***11*** → ***23*** binding sequence becomes evident as pH is increased (Figure 8). This case provides an excellent demonstration of the potential for variability among the different pathways in a highly cooperative system, in particular, variability that is not manifested in global or macro properties of the system, or even in cumulative microstate free energies. The ability of interesting and important physical features of a "simple" molecule such as human Hb to remain hidden in a global binding isotherm is an "object lesson" which may likely be applicable to a wide range of allosteric systems.

In summary, binding sequences that contribute little or no positive cooperativity to the overall binding cascade of human Hb are observed with a variety of hemesite analogs. This step-by-step development of cooperativity in the Hb cascade is revealed in the stepwise cooperative free energy

values, which yield more detailed information at the microstate level than do Hill coefficients.

REFERENCES

1. Ackers, G. K., Holt, J. M., Huang, Y., Grinkova, Y., Klinger, A. L., and Denisov, I. (2000) Confirmation of a unique intra-dimer cooperativity in the human hemoglobin $\alpha^1\beta^1$ half-oxygenated intermediate supports the Symmetry Rule model of allosteric regulation, *Proteins: Struct., Funct., Genet. Suppl. 4*, 23−43.
2. Ackers, G. K. (1998) Deciphering the molecular code of hemoglobin allostery, *Adv. Protein Chem. 51*, 185−248.
3. Ackers, G. K., Doyle, M. L., Myers, D., and Daugherty, M. A. (1992) Molecular code for cooperativity in hemoglobin, *Science 255*, 54−63.
4. Goldbeck, R. A., Esquerra, R. M., Holt, J. M., Ackers, G. K., and Kliger, D. S. (2004) The molecular code for hemoglobin allostery revealed by linking the thermodynamics and kinetics of quaternary structural change. 1. Microstate linear free energy relations, *Biochemistry 43*, 12048−12064.
5. Goldbeck, R. A., Esquerra, R. M., Kliger, D. S., Holt, J. M., and Ackers, G. K. (2004) The molecular code for hemoglobin allostery revealed by linking the thermodynamics and kinetics of quaternary structural change. 2. Cooperative free energies of $(\alpha FeCO\beta Fe)_2$ and $(\alpha Fe\beta FeCO)_2$ T-state tetramers, *Biochemistry 43*, 12065−12080.
6. Ackers, G. K., Dalessio, P. M., Lew, G. H., Daugherty, M. A., and Holt, J. M. (2002) Single residue modification of only one dimer within the hemoglobin tetramer reveals autonomous dimer function, *Proc. Natl. Acad. Sci. U.S.A. 99*, 9777−9782.
7. Holt, J. M., Klinger, A. L., Yarian, C. S., Keelara, V., and Ackers, G. K. (2005) Asymmetric distribution of cooperativity in the binding cascade of normal human hemoglobin. 1. Cooperative and noncooperative oxygen binding in Zn-substituted hemoglobin, *Biochemistry 44*, XXXXX−XXXXX.
8. Samuni, U., Juszczak, L., Dantsker, D., Khan, I., Friedman, A. J., Pérez-González-de-Apodaca, J., Bruno, S., Hui, H. L., Colby, J. E., Karasik, E., Kwiatkowski, L. D., Mozzarelli, A., Noble, R., and Friedman, J. M. (2003) Functional and spectroscopic characterization of half-liganded iron-zinc hybrid hemoglobin: evidence for conformational plasticity within the T state, *Biochemistry 42*, 8272−8288.
9. Ackers, G. K., Holt, J. M., Burgie, E. S., and Yarian, C. S. (2004) Analyzing intermediate state cooperativity in hemoglobin, in *Methods in Enzymology* (Holt, J. M., Johnson, M. J., and Ackers, G. K., Ed.) pp 3−28, Elsevier, San Diego, CA.
10. Cohn, E. J., and Edsall, J. T. (1943) *Proteins, Amino Acids and Peptides as Ions and Dipolar Ions*, Reinhold Publishing Corp., New York.
11. Edsall, J. T., and Gutfreund, H. (1983) *Biothermodynamics: The study of Biochemical Processes at Equilibrium*, John Wiley & Sons, New York.
12. Wyman, J. (1964) Linked functions and reciprocal effects in hemoglobin: a second look, *Adv. Protein Chem. 19*, 223−286.
13. Chu, A. H., Turner, B. W., and Ackers, G. K. (1984) Effects of protons on the oxygenation-linked subunit assembly in human hemoglobin, *Biochemistry 23*, 604−617.
14. Doyle, M. L., and Ackers, G. K., unpublished.
15. Huang, Y., and Ackers, G. K. (1996) Transformation of cooperative free energies between ligation systems of hemoglobin: resolution of the carbon monoxide binding intermediates, *Biochemistry 35*, 704−718.
16. Doyle, M. L., Holt, J. M., and Ackers, G. K. (1997) Effects of NaCl on the linkages between O_2 binding and subunit assembly in human hemoglobin: titration of the quaternary enhancement effect, *Biophys. Chem. 64*, 271−287.
17. Miyazaki, G., Morimoto, H., Yun, K.-M., Park, S.-Y., Nakagawa, A., Minagawa, H., and Shibayama, N. (1999) Magnesium(II) and zinc(II)-protoporphyrin IX's stabilize the lowest oxygen affinity state of human hemoglobin even more strongly than deoxyheme, *J. Mol. Biol. 292*, 1121−1136.
18. Huang, J., Juszczak, L. J., Peterson, E. S., Shannon, C. F., Yang, M., Huang, S., Vidugiris, G. V. A., and Friedman, J. M. (1999) The conformational and dynamic basis for ligand binding reactivity in hemoglobin Ypsilanti (β99 Asp → Tyr): origin of the quaternary enhancement effect, *Biochemistry 38*, 4514−4525.
19. Doyle, M. L., Lew, G., Turner, G. J., Rucknagel, D., and Ackers, G. K. (1992) Regulation of oxygen affinity by quaternary enhancement: does hemoglobin Ypsilanti represent an allosteric intermediate? *Proteins: Struct., Funct., Genet. 14*, 351−362.
20. Ackers, G. K., and Johnson, M. L. (1990) Analysis of hemoglobin oxygenation from combined equilibrium and kinetic data. Is quaternary enhancement necessary?, *Biophys. Chem. 37*, 265−279.
21. Mills, F. C., and Ackers, G. K. (1979) Quaternary enhancement in binding of oxygen by human hemoglobin, *Proc. Natl. Acad. Sci. U.S.A. 76*, 273−277.
22. Holt, J. M., and Ackers, G. K. (1995) The pathway of allosteric control as revealed by hemoglobin intermediate states, *FASEB J. 9*, 210−218.
23. Kavanaugh, J. S., Chafin, D. R., Arnone, A., Mozzarelli, A., Claudio, R., Rossi, G. L., Kwiatkowski, L. D., and Noble, R. W. (1995) Structure and oxygen affinity of crystalline desArg141-α human hemoglobin A in the T state, *J. Mol. Biol. 248*, 136−150.
24. Daugherty, M. A., Shea, M. A., and Ackers, G. K. (1994) Bohr effects of the partially-ligated (CN-met) intermediates of hemoglobin as probed by quaternary assembly, *Biochemistry 33*, 10345−10357.

BI050710N